Supporting information for

Facile synthesis of TiO_2/Mn_3O_4 hierarchical structures for fiber-shaped flexible asymmetric supercapacitor with ultrahigh stable and tailorable performance

Rui Lin[a b], Zihan Zhu[a c], Xiang Yu [d], Ying Zhong [a], Zilong Wang [a], Shaozao Tan[b], Chuanxi Zhao*[a], Wenjie Mai*[a]

[a]Siyuan laboratory, Guangzhou Key Laboratory of Vacuum Coating Technologies and New Energy Materials, Department of Physics, Jinan University, Guangzhou, Guangdong 510632, P.R.China.

[b]Department of Chemistry, Jinan University, Guangzhou, Guangdong 510632, China

[c]Department of Materials Science and Engineering, Jinan University, Guangzhou, Guangdong 510632, China

E-mail: tcxzhao@email.jnu.edu.cn, wenjiemai@email.jnu.edu.cn

Contents:

Calculation methods

1. Electrode

Moreover, the linear capacitance (C_l) and volume capacitance (C_v) of the electrode were given and the formula (1, 2) of the CV curve is put as follows:

$$C_l = \frac{\int IdU}{L\Delta U} = \frac{S}{2Lv\Delta U_P} \tag{1}$$

$$C_V = \frac{\int IdU}{V\Delta U} = \frac{S}{2Vv\Delta U_P} \tag{2}$$

Where ΔU_P is potential window, S is the area of the closed CV curve, v is scan rate and L/V is effective linear/volume of the working electrode.

2. Device

The linear capacitance ($C_{cell\text{-}L}$) and volume capacitance ($C_{cell\text{-}V}$) of the device were calculated from the CV curves by the following formulas (3, 4):

$$C_{cell-L} = \frac{\int IdU}{L\Delta U} = \frac{S}{2Lv\Delta U_V} \tag{3}$$

$$C_{cell-V} = \frac{\int IdU}{V\Delta U} = \frac{S}{2Vv\Delta U_V} \tag{4}$$

Where ΔU_V is voltage window, S is the area of the closed CV curve, v is scan rate and L/V is effective length/volume of the device.

Additionally, the volume capacitance ($C_{cell\text{-}V}$) of the device based GCD curves can be calculated from the following equation:

$$C_{cell-V} = \frac{I\Delta t}{\Delta U_V} \tag{5}$$

Where I is the discharge current, Δt is the discharge time, ΔU_V is the voltage window. And the energy and power density could be estimated by the following formulas (6, 7):

$$E = \frac{C_{cell-V}\Delta U_V{}^2}{2V} \tag{6}$$

$$P = \frac{E}{\Delta t} \tag{7}$$

Where the $C_{cell\text{-}V}$ is the volume capacitance of the working device from formulas (5), ΔU_V is the voltage window. V is the effective volume and Δt is the discharge time of GCD curves.

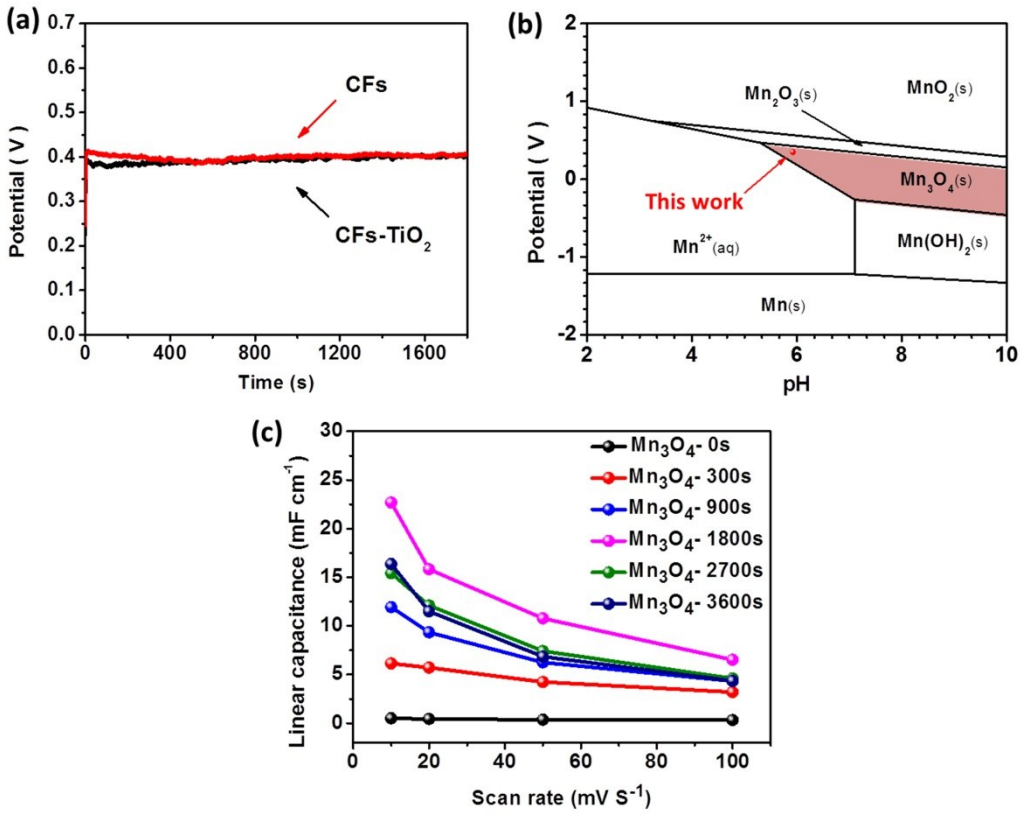

Fig. S1 (a) Voltage-time variation in electrodeposition process, which could reveal the stable voltage when applying slight current at 0.5 mA to the working electrode. (b) Pourbaix (E-pH) diagram of 0.1 M Mn−H_2O system, which shows the thermodynamic stability of possible phases and ionic species in the deposition solution at different pH values and potentials in 70 ^oC. (c) Various electrodeposition time and corresponding electrochemical performance of the electrodes.

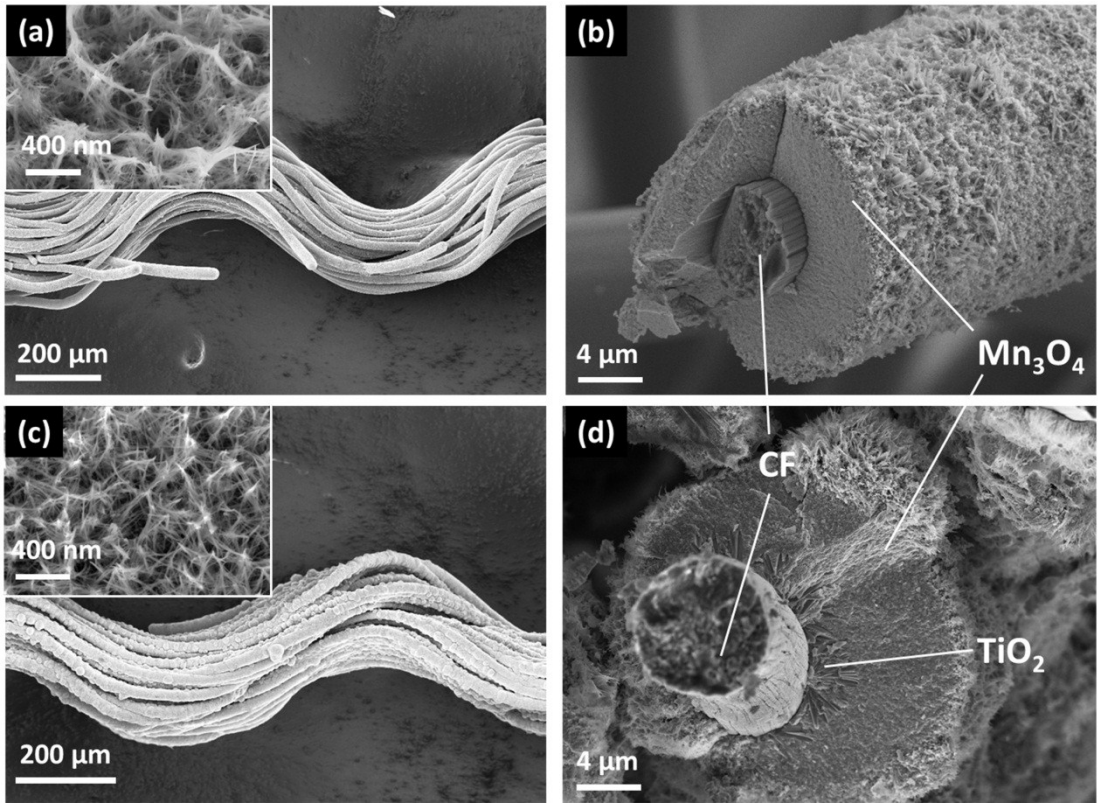

Fig. S2 SEM images of the Mn_3O_4 electrode and TiO_2/Mn_3O_4 electrode. (a) Typical image of the fiber-shaped Mn_3O_4 electronic. (b) Cross-sectional image of the Mn_3O_4 nanostructure covering on single carbon fiber. (c) SEM image of the Mn_3O_4 nanospines. (c) SEM image of the fiber-shaped TiO_2/Mn_3O_4 electronic with many typical urchin-like Mn_3O_4 nanospines. (d) Cross-sectional image of the TiO_2/Mn_3O_4 nanostructure covering on single carbon fiber.

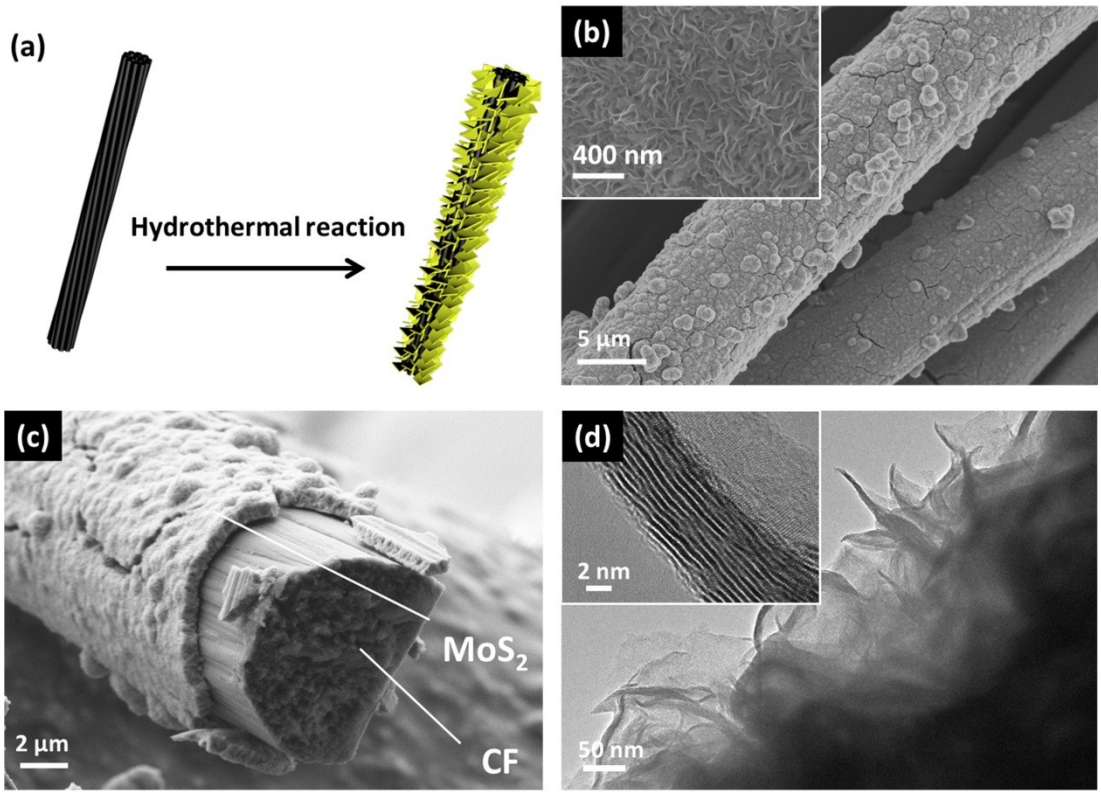

Fig. S3 (a) Schematic illustrating the synthesis procedure of MoS_2 electrode. (b) Typical image of the fiber-shaped MoS_2-coated electrode. (c) Cross-sectional image of the CF. (d) TEM image of the MoS_2 structure， insets show the typical lamellar structure of MoS_2.

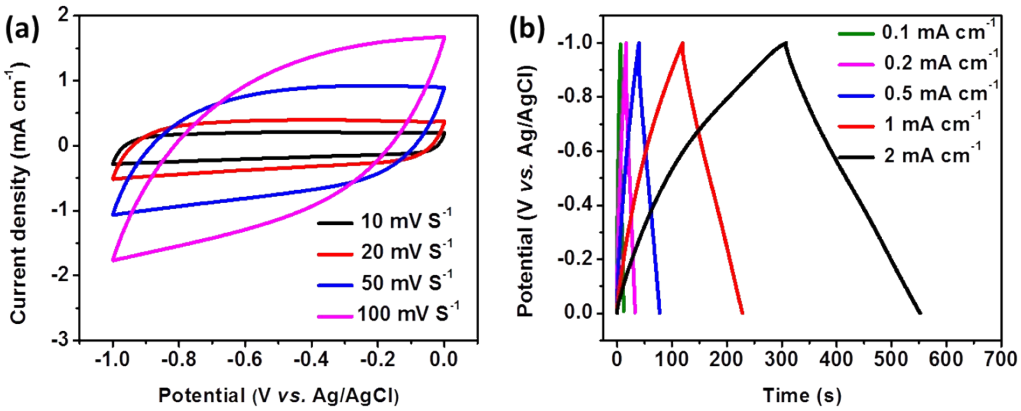

Fig. S4 (a) Different scan rates of CV curves for fiber-shaped MoS_2 electrode. (b) Galvanostatic charge/discharge curves at different current for fiber-shaped MoS_2 electrode. .

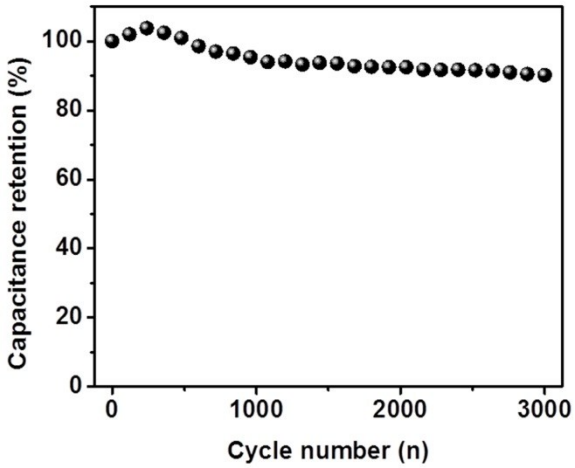

Fig. S5 Cycle stability for fiber-shaped MoS_2//TiO_2/Mn_3O_4 ASC device measured at 100 mV s^{-1}.

Table S1 Electrochemical performances of some previous fiber-shaped supercapacitors

Device configuration	Electrode material	Capacitance	Energy density	Power density	Cycle test	Time
Parallel	MnO_2	2.5 F cm^{-3}	0.22 mWh cm^{-3}	0.4 W cm^{-3}	84 % at 10000 cycles	2012 [29]
Parallel	CNT/MnO_2	25.4 F cm^{-3}	3.52 mWh cm^{-3}	127 mW cm^{-3}	n.a.	2014 [10]
Parallel	MnO_2@CNT	9.1 mF cm^{-1}	0.78 mWh cm^{-3}	20 mW cm^{-3}	84.8 % at 1000 cycles	2015 [9]
Parallel	rGO@MnO_2@PPy	12.4 F cm^{-3}	0.20 mWh cm^{-3}	150 mW cm^{-3}	92 % at 4950 cycles	2015 [13]
Parallel	MnO_2/rGO/CF//GH/CW	2.54 F cm^{-3}	0.9 mWh cm^{-3}	0.2 W cm^{-3}	90 % at 10000 cycles	2015 [28]
Parallel	N-MoO_{3-x}//MnO_2@TiN	10.3 mF cm^{-1}/ 4.1 F cm^{-3}	2.29 mWh cm^{-3}	1.64 W cm^{-3}	80.3 % at 5000 cycles	2016 [30]
Parallel	MoS_2//TiO_2/Mn_3O_4	15.28 mF cm^{-1}/19.84 F cm^{-3}	11.4 mWh cm^{-3}	2.34 W cm^{-3}	90.2 % at 3000 cycles	This work

References:

9. Pu, X.,Li, L.,Liu, M.,Jiang, C.,Du, C.,Zhao, Z.,Hu, W.; Wang, Z. L., Adv. Mater. 28 (2016) 98-105.
10. Wang, B.,Fang, X.,Sun, H.,He, S.,Ren, J.,Zhang, Y.; Peng, H., Adv Mater 27 (2015) 7854-60.
13. Huang, Y.,Hu, H.,Huang, Y.,Zhu, M.,Meng, W.,Liu, C.,Pei, Z.,Hao, C.,Wang, Z.; Zhi, C., ACS nano 9 (2015) 4766-75.
28. Zhang, Z.,Xiao, F.; Wang, S., J. Mater. Chem. A 3 (2015) 11215-11223.
29. Xiao, X.,Li, T.,Yang, P.,Gao, Y.,Jin, H.,Ni, W.,Zhan, W.,Zhang, X.,Cao, Y.,Zhong, J.,Gong, L.,Yen, W. C.,Mai, W.,Chen, J.,Huo, K.,Chueh, Y. L.,Wang, Z. L.; Zhou, J., ACS nano 6 (2012) 9200-6.
30. Yu, M.,Cheng, X.,Zeng, Y.,Wang, Z.,Tong, Y.,Lu, X.; Yang, S., Angew. Chem. 55 (2016) 6762-6.